27th EPS Conference on Contr. Fusion and Plasma Phys. Budapest, 12-16 June 2000 ECA Vol. **24B** *(2000) 416 -419*

Correlation Upper Hybrid Resonance Scattering Diagnostics of Small Scale Turbulence in FT-1 Tokamak

A.D. Gurchenko, E.Z. Gusakov, M.M. Larionov, K.M. Novik, Yu.V. Petrov, A.N. Saveliev, V.L. Selenin, A.Yu. Stepanov, V.Z. Vasiliev

Ioffe Institute, St.-Petersburg, Russia

Introduction

The Upper Hybrid Resonance (UHR) scattering is a feasible diagnostics of small scale waves and turbulence in a tokamak plasmas, possessing the merits of fine spatial resolution and enhanced scattering cross-section [1]. The UHR scattering method was used for observation of lower hybrid wave propagation in linear devices and tokamaks and for study of behavior of small scale low frequency tokamak turbulence [1]. In the last case both the Electron Temperature Gradient turbulence and small scale part of Ion Temperature Gradient turbulence are observable by the UHR scattering technique. The probing microwave is launched in this technique from the high magnetic field side of the tours as an extraordinary wave and both backscattered extraordinary wave and forward scattered ordinary wave possessing information on the correspondingly density and magnetic field fluctuations are measured. In the case of small scale fluctuations ($q > 2\omega_{ce}/c$ for Back Scattering (BS) and $q > \omega_{ce}/c$ for Cross Polarization Scattering (CPS), q is the fluctuation wavenumber) the microwave BS and CPS are localized in the vicinity of UHR determined by condition

(1) $\omega_i^2 = \omega_{pe}^2(x) + \omega_{ce}^2(x)$, where ω_i is the incident wave frequency. The spatial scan is achieved in the method by variation of probing frequency or magnetic field where as the wavenumber resolution is provided by the time of flight technique [2-4]. Unfortunately, the RADAR probing, the most suitable for investigation of broad frequency spectra [4], results not only in improvement of wavenumber resolution, but also in losses of signal to noise ratio and in high power necessary for probing.

The correlative technique proposed in [5] is free of the above drawback. It combines the merits of the cross-section enhancement with a reasonable wavenumber resolution. This technique firstly tested on linear plasma device [5] is now under development at the FT-1 tokamak. The first results obtained there are presented below.

Theoretical background

The correlative approach to the UHR scattering data analyses is based on the very local origin of the signal which is produced by different components of the turbulence spectrum in the same point. In the case of statistically homogeneous and stationary density fluctuations the cross-correlation spectrum (CCS) of two UHR scattering signals at different probing frequencies after homodyne detection is given by [5]

$$\left\langle A_s(\omega_1) A_s^*(\omega_2) \right\rangle = K(\Omega, \omega_1, \omega_2) =$$

(2)
$$= \left(\frac{\omega_1}{4\pi n_e} \right)^2 \int \left[\left|U(\vec{q})\right|^2 + \left|U(-\vec{q})\right|^2 \right] \left|\delta n_{\vec{q},\Omega}\right|^2 e^{-iq_x \Delta x_{UH}} A_i^*(\omega_2) A_i(\omega_1) \frac{d^3\vec{q}}{(2\pi)^3}$$

where $\Delta x_{UH} = x_{UH}(\omega_2) - x_{UH}(\omega_1)$ is the distance between UHR points for two probing frequencies, $\left|\delta n_{\vec{q},\Omega}\right|^2$ is the turbulence spectrum. In slab model valid in the UHR vicinity [1]

(3) $\left|U(\vec{q})\right|^2 = \rho(q_x)\left|F(q_y, q_z)\right|^2$, where $\rho(q_x)$ determining the scattering enhancement is shown in Fig.1 for parameters of the FT-1 experiment; $\left|F(q_y, q_z)\right|$ is the antenna diagram; $\left|A_i\right|^2$ is the incident power.

The fluctuation spectrum weighted with the antenna diagram

(4) $$\overline{N}^2(q_x, \Omega) = \int \left|F\right|^2 \left|\delta n_{\vec{q},\Omega}\right|^2 \frac{dq_y dq_z}{(2\pi)^2}$$

according to (3) can be obtained from the CCS by the inverse Fourier transform

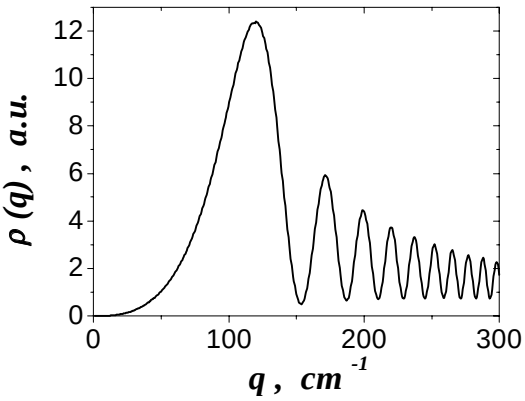

Fig.1. *The BS efficiency*

(5) $$\overline{N}^2(q_x, \Omega) = \frac{(4\pi n_e)^2}{\omega^2 \rho(q_x)} \int_{-\infty}^{+\infty} e^{iq_x \Delta x_{UH}} \frac{K(\Omega, \Delta x_{UH}) d(\Delta x_{UH})}{\left|A_i(\omega_1) A_i^*(\omega_2)\right|} \quad .$$

Experimental results

The experiment was carried out in the ohmic regime of the FT-1 tokamak (R=62.5cm, a=15cm, B=1.02T, I_p=30kA, $n_e(0)=10^{13}$cm^{-3}). The microwave probing was performed using two frequency channels in the vicinity of 28GHz. The frequency in one of them was fixed, where as it was varied from discharge to discharge in the other. The probing power down to 20mW was used. After separate homodyne detection the two signals were fed to the data acquisition system. The $\Omega/2\pi = 1.2 MHz$ component of normalized CCS $K(\Omega, \omega_2 - \omega_1)$ of these signals is shown in Fig.2a for BS experiment as a function of distance between two

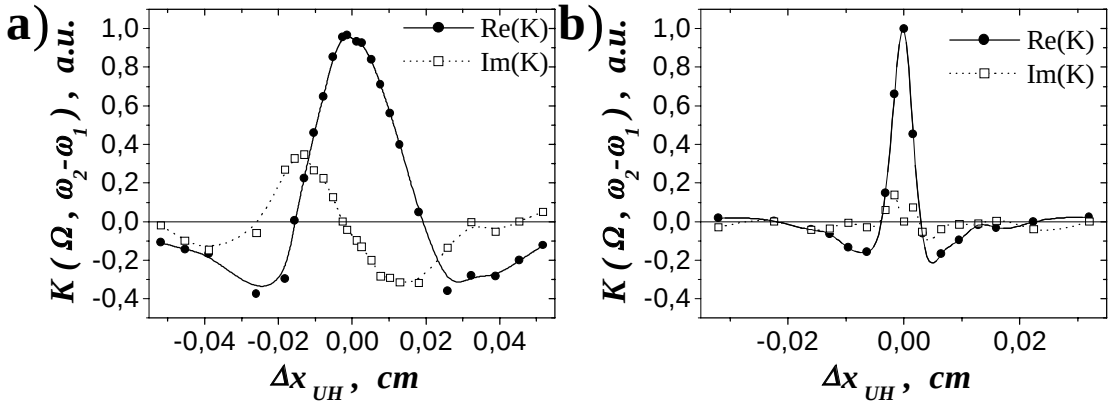

Fig.2. *The $\Omega/2\pi = 1.2 MHz$ component of normalized CCS for BS* ***(a)*** *and CPS* ***(b)***

hybrid resonances. The distance Δx_{UH} is calculated from $\omega_2 - \omega_1$ using (1). As it is seen in the figure the real part of CCS is even where as the imaginary part is the odd function of Δx_{UH}. The real part takes maximal values close to 1 for $\Delta x_{UH} \to 0$ and decreases to the noise level for Δx_{UH} =0.05cm. Both real and imaginary parts of CCS exhibits oscillations with a typical length $\Delta x_{UH} \approx 0.06$cm. The similar behavior of CCS with Δx_{UH} is demonstrated for spectral components 0.3MHz< $\Omega/2\pi$ <1.8MHz.

Dependence of CCS on Δx_{UH} for $\Omega/2\pi = 1.2 MHz$ in the case of CPS experiment is shown in Fig.2b. The imaginary part of $K(\Omega, \omega_2 - \omega_1)$ is very small, close to the noise level everywhere, where as the real part is even function of Δx_{UH}. The correlation is significant in a very narrow interval of $|\Delta x_{UH}|$<0.015cm. In spite of the fact the oscillations of the real part inside this region are not that deep as in Fig.2a, they are reproducible and statistically meaningful. After the inverse Fourier transform of dependencies shown in Fig.2a,b we obtain the q-spectra $\tilde{K}(\Omega, q_x)$, which are plotted for BS and CPS at $\Omega/2\pi = 1.2 MHz$ correspondingly in Fig.3a and Fig.3b. According to (5) $\tilde{K}(\Omega, q_x) = \left|\overline{N}_{q_x,\Omega}\right|^2 \rho(q_x)$ and should

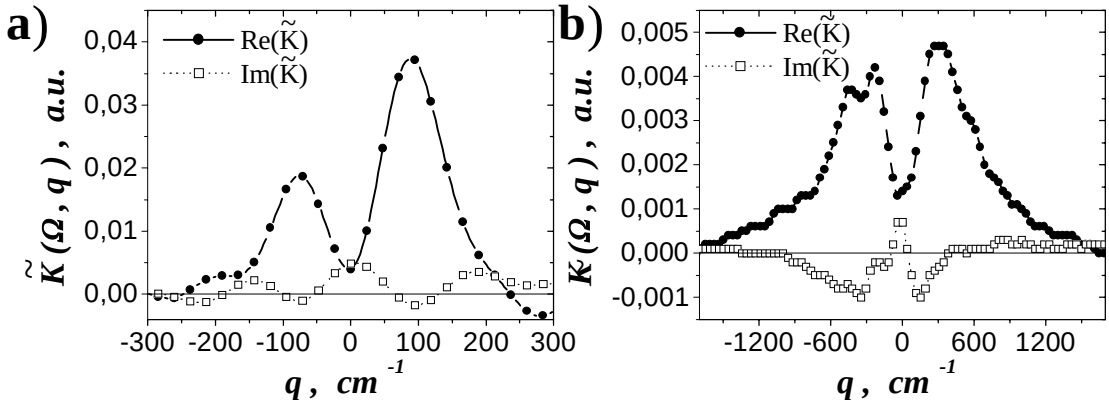

Fig.3. *The $\Omega/2\pi = 1.2 MHz$ component of the q-spectra for BS* ***(a)*** *and CPS* ***(b)***

be real. Thus, the experimental value of $\mathrm{Im}(\tilde{K})$ is giving us the accuracy of $\tilde{K}$ determination. As it is seen in Fig.3 the imaginary part of $\tilde{K}$ is much smaller than real in the case of BS ($\max \mathrm{Im}(\tilde{K}) \le 0.1 \max \mathrm{Re}(\tilde{K})$). In the case of CPS it is larger however still $\max\left|\mathrm{Im}(\tilde{K})\right| \le 0.25 \max\left|\mathrm{Re}(\tilde{K})\right|$. The dependence $\mathrm{Re}(\tilde{K}(q_x))$ is symmetric for CPS ($\tilde{K}(q) \approx \tilde{K}(-q)$) ($q \equiv q_x$) and very asymmetric for BS. In the case of BS the maximum of q-spectrum is situated at q = 100 cm^{-1} which is close to the calculated maximal value of $\rho(q)$ (see Fig.1). The value of $\tilde{K}$ is deeply suppressed for q=0, probably because the enhancement factor $\rho(q)$ scales as $\rho_{BS} \sim q^3$ in the region of q. The maximal value of $\tilde{K}$ for CPS is larger $q_m \approx 300$ cm^{-1} and the suppression for $q \to 0$ is not that deep. The possible reason for this is monotonic behavior of CPS cross-section with q_x ($\rho_{CPS} \sim q^2$) [6].

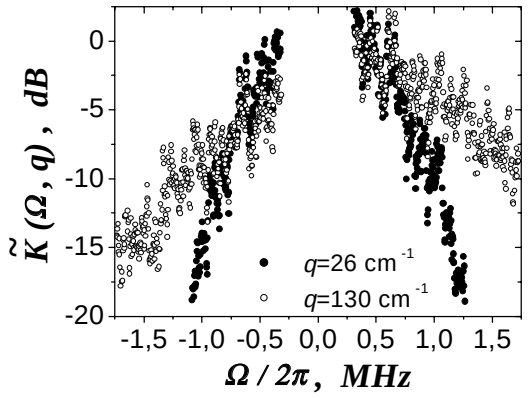

Fig.4. *The BS Ω-spectra for different q_x*

The BS CCS - $\tilde{K}(\Omega, q_x)$ are shown in Fig.4 for different q_x values. As it is seen their spectral width increases with q_x approximately linearly.

Discussion

Two possible explanations for this puzzling behavior were proposed. The first one makes use of the fact that BS takes place in the UHR in presence of strong long scale

turbulence which can modify the BS spectra due to the Doppler effect. The frequency shift of the BS signal in this case will increase linearly with q_x and the BS spectrum will give us the turbulent velocity distribution function $f(V_r)$. The rough estimation of the mean squared velocity obtained from spectra shown in Fig.4 give us a high value $4 \cdot 10^4$ cm/s, which is only a factor of 5 smaller than the poloidal rotation velocity measured in FT-1 edge $V_p = 2 \cdot 10^5$ cm/s [7].

Another interpretation of the broadening effect appeals to the ray tracing calculations [4] showing that poloidal wavenumber of the incident wave in the UHR is proportional to the radial wavenumber and initial poloidal one $k_{i\theta} \approx \eta k_{\theta 0} k_{ir}$ (see Fig.5). The density fluctuations possessing large poloidal numbers q_θ are needed for BS of such a incident wave. Supposing the linear dispersion of the fluctuation $\Omega = V q_\theta$, which is the case for plasma solid rotation or for the drift turbulence, and taking into account the BS Bragg condition $q_\theta = 2k_{i\theta}$; $q_r = 2k_{ir}$, we obtain the frequency shift of the BS wave as $\Omega = 2\eta V k_{\theta 0} k_{ir} = \eta V k_{\theta 0} q_r$. The form of the scattering spectrum in this interpretation is determined by the antenna diagram $\left|F(q_y, q_z)\right|^2$. The estimation of the phase velocity V from the experimental data gives $V = 2.6 \cdot 10^6$ cm/s, where as the diamagnetic drift velocity calculated for the UHR position is $V_d = 10^6$ cm/s.

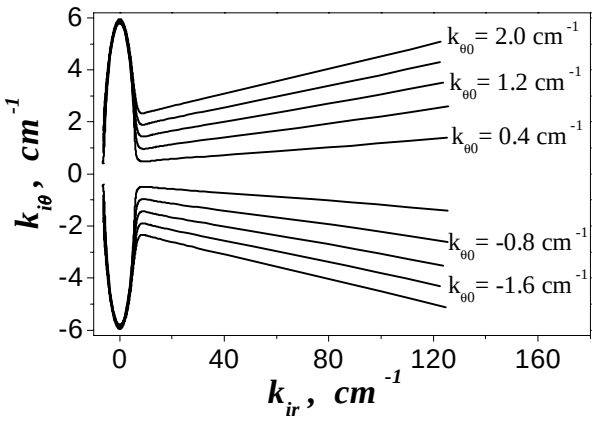

Fig.5. *The dependence of poloidal wavenumber of the incident wave $k_{i\theta}$ on the radial wavenumber k_{ir} for different initial poloidal wavenumbers $k_{\theta 0}$*

In spite of the fact both above mechanisms taken separately are facing problems, when acting simultaneously they can explain the BS spectra features.

Conclusions

The correlation UHR scattering scheme is shown to be capable to provide the wave number resolved measurements in agreement with the recently reported RADAR measurement [4]. Unlike the RADAR scheme which was tested at 10W probing power it benefits from the cross section enhancement in the UHR and operates at 20mW probing power level.

Acknowledgement

The paper was supported by RFBR grant 98-02-18348, INTAS grant 97-11018 and by Contract of Ministry of Science of Russia.

References

1. K.M. Novik, A.D. Piliya, Plasma Phys. Contr. Fusion, 1994, **36**, 357.
2. V.I. Arkhipenko et al., Plasma Phys. Contr. Fusion 1995, **37A**, 347.
3. D.G. Bulyginskiy et al., Cont. Papers 25th EPS Conf. on CFPP Prague, 1998, **22C**, 1546.
4. A.D. Gurchenko et al., Cont. Papers 26th EPS Conf. on CFPP Maastricht, 1999, **23J**, 37.
5. V.I. Arkhipenko, V.N. Budnikov, E.Z. Gusakov, Tech. Phys. Lett. 1993, **19**, 20.
6. E.Z. Gusakov, Proc 25th Conf. CFPP Prague, 1998, **22C**, 39.
7. D.G. Bulyginskiy et al., Plasma Phys. Controlled Nuclear Fusion Research, 1984, **1**, 491.